

Polarisation statistics of vector scattering matrices from the circular orthogonal ensemble

Niall Byrnes, Matthew R. Foreman¹

Blackett Laboratory, Department of Physics, Imperial College London, Prince Consort Road, London SW7 2AZ, United Kingdom

Abstract

We study the polarisation properties of random $N \times N$ scattering matrices distributed according to the circular orthogonal ensemble. We interpret 2×2 sub-blocks of the scattering matrix as Jones matrices and study their statistical properties. Using the polar decomposition, we derive probability density functions for retardance and diattenuation from scattering matrices of arbitrary size and in the limit $N \rightarrow \infty$.

Keywords: Random matrix theory, vector scattering matrix, disordered media, retardance, diattenuation

1. Introduction

Polarised light is widely used in a variety of optical technologies, such as in characterising the optical properties of thin films [1], measuring magnetic fields of astronomical objects [2], determining the orientation of single molecules [3], readout of multiplexed optical data storage [4] and discriminating healthy and precancerous tissue [5]. When fully polarised coherent light passes through a disordered medium or is reflected by a rough dielectric surface, scattering leads to scrambling of the incident signal and the formation of a complex speckle pattern [6]. In addition to intensity, the state of polarisation can also exhibit significant spatial variation throughout a speckle pattern [7]. Furthermore, for any given measurement point, the polarisation state of the scattered field can vary unpredictably between different realisations of the scattering medium, or over time in the case of a dynamic medium. In principle, the exact morphology of a speckle pattern is a deterministic fingerprint of the microscopic configuration of the scattering medium. In practice, however, speckle patterns are essentially random and statistical methods offer the most pragmatic approach to their study.

A plethora of tools exist to describe polarised light. For example, Stokes parameters constitute a set of four measurable quantities that characterise the polarisation state of light at a fixed point in space [8]. The statistical properties of these quantities are well known, particularly in the case of underlying Gaussian fields [9–15], and have found use in the analysis of surface roughness [16, 17] and in remote sensing [18]. The Mueller matrix, which describes the linear transformation of the Stokes parameters upon interaction with

¹Corresponding author: matthew.foreman@imperial.ac.uk

a scattering medium, has also been studied extensively and can reveal important structural information about scattering media [19–21]. Among the numerous techniques used to analyse Mueller matrices, the polar decomposition is notably popular as it expresses a Mueller matrix as a series of components that have intuitive optical interpretations, namely a diattenuator, retarder and depolariser [22]. The statistical properties of these components have found application in, for example, aiding early cancer diagnostics [23–25].

More recently, polarisation-sensitive transmission and reflection matrices for random media have been experimentally measured [26–28]. These matrices describe the response of a medium to an arbitrary incident wavefront, typically generated using a spatial light modulator. Transmission and reflection matrices, which are sub-blocks of the scattering matrix, are amenable to theoretical study using random matrix theory in which a scattering matrix is randomly sampled from a matrix ensemble defined by symmetry constraints [29]. Random matrix theory has revealed universal properties of scattering media, such as the existence of open eigenchannels: incident wavefronts that are highly transmitting, even in circumstances in which the ballistic signal has fully decayed [30]. While the theory of random matrices is a mature subject, particularly in its applications in mesoscopic quantum physics [31], its application to the scattering of polarised light remains relatively unexplored. In this work, we explore the polarisation properties of random scattering matrices using one of the earliest proposed random matrix models: the circular ensembles. In particular, we look to bridge the gap between random scattering matrices and the statistics of more traditional polarimetric quantities, such as diattenuation and retardance.

In Section 2 we briefly discuss the scattering matrix appropriate for polarised light, its physical interpretation and mathematical constraints. We then introduce the circular orthogonal ensemble as a statistical model for the scattering matrix and explore its predictions. In Section 3 we examine the polar decomposition and derive probability distributions for diattenuation and retardance. We conclude with a summary of our findings in Section 4.

2. The Scattering Matrix

We begin with a brief overview of the scattering matrix. For a linear system, the scattering matrix \mathbf{S} relates the field components of waves that impinge upon the system to those that are scattered away from the system. Scattering matrices provide a useful description for a number of different types of systems, such as multi-mode fibers [32] and photonic networks [33]. For concreteness, we shall focus our attention on the example of plane wave scattering by a medium with slab geometry, details of which can be found in Ref. [34].

The incident and scattered fields in the regions either side of a scattering slab can be expressed using the angular spectrum decomposition [8]. Suppose that these angular spectra can be well-approximated by discrete spectra consisting of M plane wave components. We shall take M to be arbitrary, but one can imagine that complete information of the fields is obtained in the limit $M \rightarrow \infty$. In the far-field of the scattering medium, the field associated with each plane wave component is transverse to the corresponding wavevector [35]. The polarisation state of each plane wave component can therefore be described using a pair of orthogonal field components, which together form a Jones vector. The scattering matrix, which can be expressed as a 2×2 block matrix of reflection and transmission matrices, describes the coupling between the full set of incident and outgoing plane wave components.

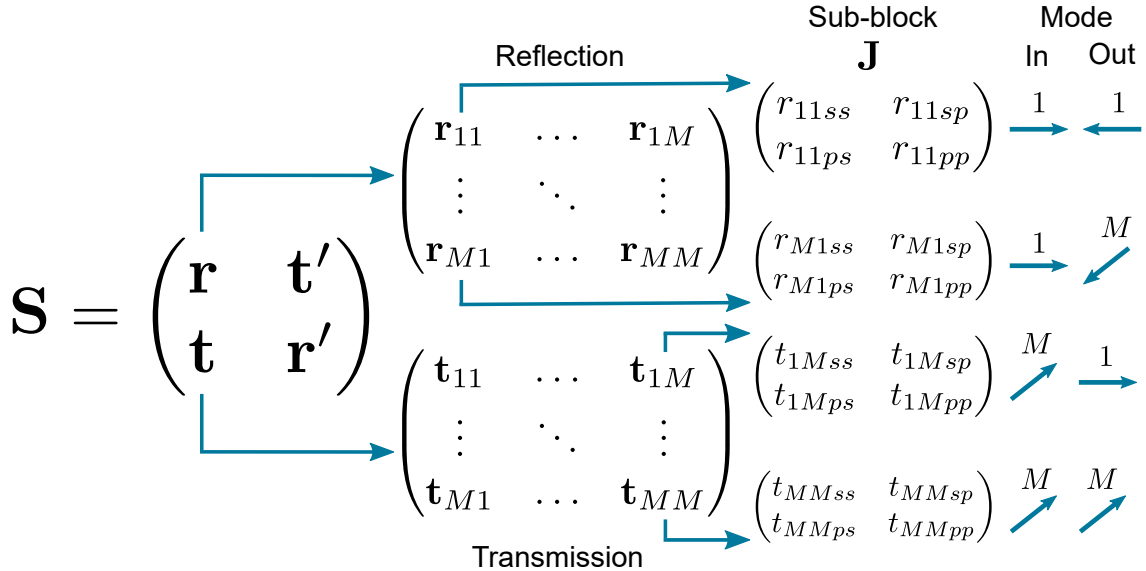


Figure 1: A schematic diagram outlining the block structure of the scattering matrix. The transmission and reflection matrix each consist of M^2 sub-blocks of size 2×2 . Each sub-block can be interpreted as a Jones matrix, which describes the scattering between a pair of plane wave components in the incident and scattered field.

65 When the polarisation state of each plane wave is accounted for, we can think of the transmis-
sion (reflection) matrix as consisting of many (M^2) 2×2 sub-blocks, each of which describes
the transmission (reflection) between a pair of plane wave components in the incident and
outgoing fields. It is the structure of these 2×2 sub-blocks that encode the polarimetric
70 sub-blocks as Jones matrices. As there are a total of M plane wave components, the transmis-
sion and reflection matrices are of size $2M \times 2M$ and, consequently, the scattering matrix
is of size $4M \times 4M$. An outline of the structure of the scattering matrix is shown in Figure
1. We use the notation \mathbf{t}_{ij} and \mathbf{r}_{ij} for $1 \leq i, j \leq M$ to refer to the different sub-blocks
75 within the transmission and reflection matrices \mathbf{t} and \mathbf{r} . Within an arbitrary sub-block \mathbf{J} ,
the subscripts s and p are used to denote two orthogonal basis polarization states. On the
far right of Figure 1 we also demonstrate some examples of pairings of incident and scattered
wavevectors.

In order to choose a suitable statistical model for the scattering matrix, it is important
to consider the mathematical constraints it obeys. Following Ref. [34], it is known that,
when the scattering matrix is appropriately normalised, conservation of energy is equivalent
to unitarity, i.e. $\mathbf{S}^\dagger \mathbf{S} = \mathbf{I}$, where \dagger denotes the conjugate transpose and \mathbf{I} is the identity
matrix. In addition, if reciprocity (or time reversal symmetry) holds, then \mathbf{S} obeys

$$\mathbf{S} = \mathbf{K} \mathbf{S}^T \mathbf{K}^{-1}, \quad (1)$$

where $\mathbf{K} = \mathbf{I}_2 \otimes \boldsymbol{\Sigma} \otimes \boldsymbol{\sigma}_z$. Here, \mathbf{I}_2 is the 2×2 identity matrix; $\boldsymbol{\Sigma}$ is the $M \times M$ exchange
matrix containing 1s on its anti-diagonal and 0s elsewhere; $\boldsymbol{\sigma}_z = \text{diag}(1, -1)$ is a Pauli matrix
80 and \otimes denotes the Kronecker product. By the symmetry of \mathbf{K} , the reciprocity (time reversal
symmetry) constraint can be rewritten as $\mathbf{S} \mathbf{K} = \mathbf{K} \mathbf{S}^T = (\mathbf{S} \mathbf{K})^T$, from which it is evident that
the matrix $\mathbf{S} \mathbf{K}$, which is a signed permutation of \mathbf{S} , is symmetric. Since \mathbf{K} is unitary, it also

follows that \mathbf{SK} is unitary. One can therefore generate a random scattering matrix satisfying Eq. (1) by first generating a random unitary, symmetric matrix \mathbf{S}' and then computing $\mathbf{S} = \mathbf{S}'\mathbf{K}$, which is equivalent to performing a signed permutation of the elements of \mathbf{S}' .

One of the simplest random matrix ensembles for unitary, symmetric matrices is the circular orthogonal ensemble (COE(N), where N denotes the size of the matrix). In the COE, \mathbf{S}' can be generated by first randomly sampling a unitary matrix \mathbf{U} uniformly from the unitary group and then computing $\mathbf{S}' = \mathbf{U}^T\mathbf{U}$. For more mathematical details, we refer the interested reader to Ref. [36]. Intuitively, matrices generated from the COE describe isotropic scattering media, i.e. systems that scatter equally into all outgoing modes. The COE may therefore be an appropriate model for systems that are comparably transmissive and reflective. In addition, the COE has also been used as a model for the reflection matrix alone in the case of very thick media for which transmission is negligible [37].

To study the polarisation properties of \mathbf{S} , we shall consider the joint statistics of 2×2 sub-blocks of \mathbf{S} , which we view as Jones matrices as per the previous discussion. Suppose that \mathbf{S} is an $N \times N$ matrix ($N = 4M$) sampled as previously discussed and let \mathbf{J} be an arbitrary 2×2 sub-block of \mathbf{S} . Due to reciprocity, sub-blocks that lie on the anti-diagonals of the reflection matrices satisfy $\mathbf{J} = \boldsymbol{\sigma}_z \mathbf{J}^T \boldsymbol{\sigma}_z$, which is equivalent to the condition $J_{12} = -J_{21}$. These sub-blocks correspond to back-scattering in the direction opposite to the incident wavevector. Consequently, the statistics of these sub-blocks differ to those of other Jones matrices located elsewhere within the scattering matrix. Therefore, in order to conveniently account for both types of sub-block, we introduce a parameter α , analogous to the more common β symmetry parameter [29], which we set equal to 1 for back-scattering Jones matrices and 2 for all other Jones matrices.

Moments of the elements of \mathbf{S} follow straightforwardly from moments of the elements of COE matrices, which are well-known. We have $\langle J_{ij} \rangle = 0$ for $1 \leq i, j \leq 2$, regardless of α , and

$$\langle J_{ij} J_{kl}^* \rangle_{\alpha=1} = \frac{\delta_{ik} \delta_{jl} (1 + 2\delta_{ij}) - \delta_{il} \delta_{jk}}{N + 1}, \quad \langle J_{ij} J_{kl}^* \rangle_{\alpha=2} = \frac{\delta_{ik} \delta_{jl}}{N + 1}, \quad (2)$$

where the averages are taken over COE(N) [38]. The increased correlation for diagonal elements in the $\alpha = 1$ case of Eq. (2) is understood to be a manifestation of the coherent backscattering effect [29]. Every Jones matrix has a corresponding Mueller-Jones matrix and, by averaging these Mueller-Jones matrices over different realisations of the scattering matrix, one can obtain an ensemble average Mueller matrix $\langle \mathbf{M} \rangle$ associated with each 2×2 sub-block of \mathbf{S} [39]. From Eq. (2) we see that for $\alpha = 2$, elements of \mathbf{J} are uncorrelated, meaning the average Mueller matrix associated with the ensemble of \mathbf{J} matrices is that of a pure depolariser, i.e. $\langle \mathbf{M} \rangle \sim \text{diag}(1, 0, 0, 0)$. It is worth emphasising here that for a given scattering matrix and incident field, the scattered field is fully polarised. The average Stokes vector of the scattered field, however, is that of fully depolarised light, irrespective of the incident field. In fact, we found numerically that for any incident polarisation state, the polarisation states of the scattered field for different scattering matrix realisations are distributed uniformly over the Poincaré sphere.

For $\alpha = 1$, we found instead that $\langle \mathbf{M} \rangle \sim \text{diag}(1, \frac{1}{3}, -\frac{1}{3}, \frac{1}{3})$. In this case, the average Mueller matrix is a partial depolariser, which reduces the degree of polarisation of any fully polarised incident state to $1/3$. The retention of some degree of polarisation can be under-

stood by noting that the squared absolute values of the diagonal elements of \mathbf{J} are, on average, twice as large as those of the off-diagonal terms. Thus, there is a slight preference for the scattered polarisation state to be parallel to the incident polarisation state. Numerical tests
125 showed that for any incident polarisation state, the distribution of the scattered polarisation states on the Poincaré sphere peaks at the incident polarisation state, about which it spreads symmetrically.

We finally note that regardless of the position of the Jones matrix within the scattering matrix, no polarisation states, on average, scatter with any unique behaviour not exhibited
130 by any other polarisation states. The COE is therefore unable to account for phenomena such as the polarisation memory effect for circularly polarised light, where circularly polarised light tends to retain its degree of polarisation over greater distances than linearly polarised light, particularly in anisotropic scattering environments [40].

3. Diattenuation and Retardance

While the COE shows no bias for any particular polarisation state, we found that diattenuation and retardance associated with Jones matrices within the scattering matrix follow non-trivial probability distributions. The remainder of this report is devoted to their analysis. Diattenuation and retardance for an arbitrary Jones matrix can be defined through the polar decomposition. Any Jones matrix \mathbf{J} may be factorised as

$$\mathbf{J} = \mathbf{J}_R \mathbf{J}_D, \quad (3)$$

where $\mathbf{J}_D = \sqrt{\mathbf{J}^\dagger \mathbf{J}}$ is a positive semi-definite Hermitian (diattenuator) matrix and $\mathbf{J}_R = \mathbf{J} \mathbf{J}_D^{-1}$ is a unitary (retarder) matrix [41]. We note that \mathbf{J} also admits a reverse polar decomposition $\mathbf{J} = \mathbf{J}'_D \mathbf{J}'_R$, where $\mathbf{J}'_D = \sqrt{\mathbf{J} \mathbf{J}^\dagger}$. For our purposes, either choice of polar decomposition leads to the same results and we shall hence proceed with that of Eq. (3). The diattenuation D and retardance R of \mathbf{J} are defined by²

$$D = \frac{|s_1^2 - s_2^2|}{s_1^2 + s_2^2}, \quad R = \min(|\theta_1 - \theta_2|, 2\pi - |\theta_1 - \theta_2|), \quad (4)$$

135 where s_1 and s_2 are the eigenvalues of \mathbf{J}_D and $\exp(i\theta_1)$ and $\exp(i\theta_2)$ are the eigenvalues of \mathbf{J}_R . Note that s_1 and s_2 are also the singular values of \mathbf{J} . The eigenvector of \mathbf{J}_D with largest eigenvalue, when viewed as a unit vector on the Poincaré sphere, is known as the diattenuation vector [22]. Similarly, the eigenvector of \mathbf{J}_R corresponding to the polarisation state that experiences the shortest optical path length is known as the retardance vector. Generally
140 speaking, diattenuation is a measure of the extent to which the transmission (reflection) of light by a system depends on the incident polarisation state. When $D = 0$, all incident polarisation states are transmitted (reflected) equally and when $D = 1$, \mathbf{J} is singular and there exists a polarisation state for which the transmission (reflection) is zero. Similarly, retardance can be thought of as a measure of the extent to which the optical path length
145 of a system depends on the incident polarisation state. We emphasise here that since \mathbf{S} is

²Our expression for retardance is slightly non-standard, but ensures that $0 \leq R \leq \pi$ for unordered θ_1 and θ_2 .

assumed to be unitary, we are only concerned with scattering-induced diattenuation and not dichroism due to polarisation-dependent absorption. A low output intensity in one particular plane wave component must be compensated by a larger output intensity in another plane wave component so that energy is conserved overall.

We found that the statistical properties of diattenuation and retardance are identical for sub-blocks within both \mathbf{S} and \mathbf{S}' , i.e. they are unaffected by the signed permutation matrix \mathbf{K} . For simplicity, we shall therefore henceforth take \mathbf{S} to be a symmetric, unitary matrix sampled directly from the COE. The $\alpha = 1$ case corresponds to sub-blocks lying on the diagonal of \mathbf{S} , which are symmetric 2×2 matrices. For on-diagonal Jones matrices of \mathbf{S} , the joint probability density function for the elements of \mathbf{J} was derived in Ref. [42]. For off-diagonal Jones matrices, we found numerically that for large values of N , such matrices are statistically similar to arbitrary 2×2 sub-blocks of uniformly distributed unitary matrices (without a symmetry constraint). As shall be demonstrated, we found that this approximation works reasonably well even for values as small as $N = 12$ ($M = 3$). The $N \times N$ unitary group sampled with uniform probability density is known as the circular unitary ensemble (CUE(N)), and the probability density function for an arbitrary 2×2 sub-block of a matrix sampled from CUE(N) has also been derived, such as in Ref. [43]. Combining these two results, the probability density function for \mathbf{J} is given by (approximately in the $\alpha = 2$ case)

$$p(\mathbf{J}) \propto [\det(\mathbf{I} - \mathbf{J}^\dagger \mathbf{J})]^{\alpha(N-6+\alpha)/2}. \quad (5)$$

150 We note that the density in Eq. (5) is independent of the choice of polarisation basis, since it is invariant under the transformation $\mathbf{J} \rightarrow \mathbf{U}\mathbf{J}\mathbf{U}^{-1}$ for all 2×2 unitary matrices \mathbf{U} .

The polar decomposition is closely related to the singular value decomposition, in which \mathbf{J} is factorised as

$$\mathbf{J} = \begin{cases} \mathbf{U}\mathbf{\Sigma}\mathbf{U}^\text{T} & \text{if } \alpha = 1, \\ \mathbf{V}\mathbf{\Sigma}\mathbf{W}^\dagger & \text{if } \alpha = 2, \end{cases} \quad (6)$$

where \mathbf{U} , \mathbf{V} and \mathbf{W} are unitary matrices containing the singular vectors of \mathbf{J} and $\mathbf{\Sigma} = \text{diag}(s_1, s_2)$ [44]. In the case $\alpha = 1$, we have used a special version of the singular value decomposition known as the Autonne-Takagi factorisation, which is possible due to the sym-
155 metry of \mathbf{J} . Straightforward algebra shows that the diattenuator and retarder matrices of Eq. (3) are given by $\mathbf{J}_D = \mathbf{U}^* \mathbf{\Sigma} \mathbf{U}^\text{T}$, $\mathbf{J}_R = \mathbf{U} \mathbf{U}^\text{T}$ for $\alpha = 1$ and $\mathbf{J}_D = \mathbf{W} \mathbf{\Sigma} \mathbf{W}^\dagger$, $\mathbf{J}_R = \mathbf{V} \mathbf{V}^\dagger$ for $\alpha = 2$. It can thus be seen that the diattenuation and retardance vectors are closely related to the singular vectors of \mathbf{J} .

Let us now express the density for \mathbf{J} in Eq. (5) in terms of the variables used in Eq. (6). Doing so requires computing the Jacobian for the change of variables. Letting $d\mathbf{J}$ denote the product of the differentials of the elements of \mathbf{J} , we find that

$$p(\mathbf{J})d\mathbf{J} \propto s_1 s_2 |s_1^2 - s_2^2|^\alpha [(1 - s_1^2)(1 - s_2^2)]^{\alpha(N-6+\alpha)/2} ds_1 ds_2 d\mu(\mathbf{U}, \mathbf{V}, \mathbf{W}), \quad (7)$$

where $d\mu(\mathbf{U}, \mathbf{V}, \mathbf{W}) = d\mu(\mathbf{U})$ for $\alpha = 1$; $d\mu(\mathbf{V})d\mu(\mathbf{W})$ for $\alpha = 2$ and $d\mu$ is the invariant
160 (Haar) measure for the unitary group. In deriving Eq. (7), we have made use of the fact that $\det(\mathbf{I} - \mathbf{J}^\dagger \mathbf{J}) = \det(\mathbf{I} - \mathbf{\Sigma}^\dagger \mathbf{\Sigma}) = (1 - s_1^2)(1 - s_2^2)$. Observing the right hand side of Eq. (7), we note that the singular values and singular vectors of \mathbf{J} are statistically independent, and the

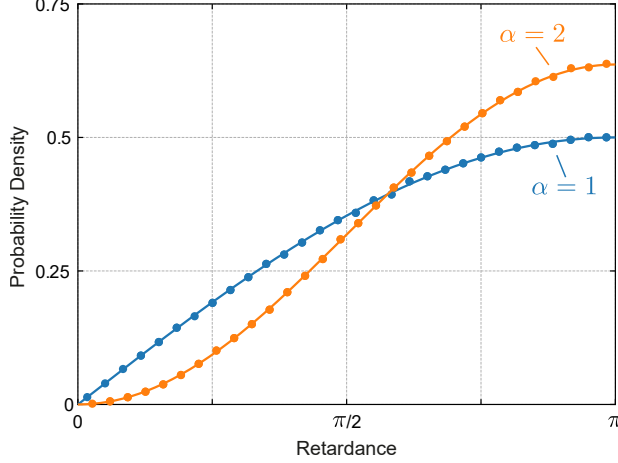


Figure 2: Histograms of retardance for on-diagonal sub-blocks ($\alpha = 1$) and off-diagonal sub-blocks ($\alpha = 2$). Data points were calculated from 10^6 realisations of COE matrices. Fitting curves are given by Eq. (10).

joint probability density function for s_1 and s_2 is proportional to the function multiplying the differentials. In addition, we see that the matrices \mathbf{U} , \mathbf{V} and \mathbf{W} are all uniformly distributed unitary matrices, irrespective of N . It follows that the diattenuation and retardance vectors are uniformly distributed on the surface of the Poincaré sphere, meaning there are no preferentially transmitted (reflected) polarisation states across the entire ensemble of scattering matrices.

We now derive probability density functions for R and D . For $\alpha = 1$, we see that $\mathbf{J}_R = \mathbf{U}\mathbf{U}^T$ is distributed according to COE(2). For $\alpha = 2$ on the other hand, $\mathbf{J}_R = \mathbf{V}\mathbf{W}^\dagger$ is the product of two uniformly distributed unitary matrices and is thus distributed according to CUE(2). Notably, there is no N dependence on the statistics of the retarder matrix in either case. The joint density for the eigenvalues of \mathbf{J}_R is given by [45]

$$p(\theta_1, \theta_2) \propto |e^{i\theta_1} - e^{i\theta_2}|^\alpha. \quad (8)$$

The probability density function for the retardance can therefore be computed by the integral

$$p(R) \propto \int_0^{2\pi} \int_0^{2\pi} |e^{i\theta_1} - e^{i\theta_2}|^\alpha \delta[R - \min(|\theta_1 - \theta_2|, 2\pi - |\theta_1 - \theta_2|)] d\theta_1 d\theta_2, \quad (9)$$

where δ is the Dirac delta function. From Eq. (9), we can make the change of variables $x = \theta_2 - \theta_1$, $y = \theta_2 + \theta_1$ and evaluate the integral piecewise, yielding

$$p(R) = \begin{cases} \frac{1}{2} \sin(\frac{R}{2}) & \text{if } \alpha = 1, \\ \frac{2}{\pi} \sin^2(\frac{R}{2}) & \text{if } \alpha = 2, \end{cases} \quad (10)$$

which we have plotted as solid lines in Figure 2. The data points (circles in Figure 2) were calculated by randomly generating 10^6 COE matrices and calculating R according to Eq. (4) from two different sub-blocks of \mathbf{S} : one on-diagonal and one off-diagonal. As can be seen, the theoretical curves fit the data points excellently. In both cases we see that the density is monotonically increasing and peaks at $R = \pi$. Therefore, in terms of relative phase changes

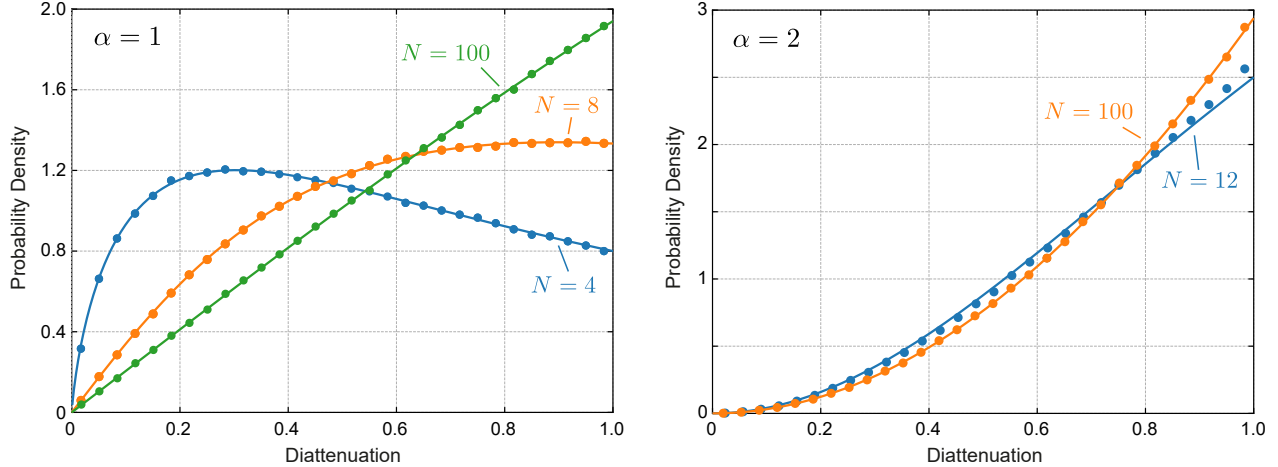


Figure 3: Histograms of diattenuation for sub-blocks of scattering matrices of different sizes. Data points were calculated from 10^6 realisations of COE matrices. Fitting curves are given by Eq. (13).

experienced by the incident field, the scattering medium is most likely to behave as a half-wave plate. We note that our result here for $\alpha = 2$ is similar to that derived elsewhere for the retardation angle in optical fibres using a random Jones matrix model, albeit using a slightly different definition for retardance [46].

The probability density function for the diattenuation can be found by integrating the joint density for s_1 and s_2 in Eq. (7). Explicitly, we have

$$p(D) \propto \int_0^1 \int_0^1 s_1 s_2 |s_1^2 - s_2^2|^\alpha [(1 - s_1^2)(1 - s_2^2)]^{\alpha(N-6+\alpha)/2} \delta\left(D - \frac{|s_1^2 - s_2^2|}{s_1^2 + s_2^2}\right) ds_1 ds_2, \quad (11)$$

which, after some manipulation, can be reduced to

$$p(D) \propto \frac{D^\alpha}{(1+D)^{\alpha+2}} \int_0^1 x^{\alpha+1} \left[(1-x) \left(1 - \frac{1-D}{1+D} x\right) \right]^{\alpha(N-6+\alpha)/2} dx. \quad (12)$$

The resulting integral in Eq. (12) can be expressed in terms of the hypergeometric function ${}_2F_1$ (see 3.197, 3. of Ref [47]). After normalising the resulting densities, we find that

$$p(D) = \begin{cases} 16 \frac{N-2}{N+1} \frac{D}{(1+D)^3} {}_2F_1\left(\frac{5-N}{2}, 3; \frac{N+3}{2}; \frac{1-D}{1+D}\right) & \text{if } \alpha = 1, \\ 48 \frac{N-2}{N} \frac{D^2}{(1+D)^4} {}_2F_1\left(4-N, 4; N+1; \frac{1-D}{1+D}\right) & \text{if } \alpha = 2. \end{cases} \quad (13)$$

Some example plots of these densities for different values of N are shown in Figure 3 for both $\alpha = 1$ and $\alpha = 2$. As with our retardance calculations, the data points were computed with Eq. (4) using 10^6 realisations of COE matrices for each matrix size. Our result for $\alpha = 1$ is exact and fits very well for all matrix sizes. For $\alpha = 2$, our approximate result fits the data reasonably well for $N \geq 12$. While not shown here, for $N < 12$ we observed deviations from the simulated data, particularly in the minimal case $N = 4$, which corresponds to single-mode scattering. As N increases however, the approximation improves.

As can be seen, with the exception of $N = 4$ for $\alpha = 1$, the densities are strictly increasing and peak at $D = 1$ for all values of N . We therefore find that, when viewing the

outgoing field in a single mode, it is most probable that the scattering medium behaves like a polarising filter that totally rejects one polarisation state. Since the diattenuation vector is uniformly distributed on the Poincaré sphere, the polarisation state that is rejected is completely random. Furthermore, since different sub-blocks of \mathbf{S} are uncorrelated, the rejected polarisation states in different outgoing modes are also uncorrelated. Since the diattenuation and retardance statistics are independent, we conclude that the most probable behaviour of a Jones matrix within the scattering matrix is that of a polarizing filter followed by a half-wave plate, both with randomly oriented and independent eigenvectors. We note that the mean diattenuation is lower for the $\alpha = 1$ case. When diattenuation is large, the scattered polarisation state tends to be close to the diattenuation vector, regardless of the incident polarisation state. This would result in a loss of correlation between the incident and scattered polarisation states. As discussed in the previous section, we found that the incident and scattered polarisation states were partially correlated in the back-scattering direction, which is therefore consistent with a lower average diattenuation.

In optical scattering experiments, the number of modes admitted by a system tends to be very large, typically on the order of tens of millions per millimetre of illuminated surface area for visible light [48]. It is therefore useful to consider the large N limit of Eq. (13). This limit may be taken directly using the asymptotic relation

$${}_2F_1(a - N, b; c + N; z) \sim \frac{1}{(1 + z)^b}, \quad (14)$$

which holds for large N and arbitrary a, b and c [49]. Applying this result to Eq. (13) and renormalising the resulting densities, we find the simple results

$$p(D)_{N \rightarrow \infty} = \begin{cases} 2D & \text{if } \alpha = 1, \\ 3D^2 & \text{if } \alpha = 2. \end{cases} \quad (15)$$

Observing again Figs. 2 and 3, these asymptotic densities closely match the densities for $N = 100$, which is well below the number of modes expected in a typical scattering experiment. Interestingly, Eq. (15) can also be derived using a Gaussian approximation for the elements of the Jones matrix. Details of this calculation can be found in Appendix A. A summary of the mean, variance, skewness and kurtosis of the densities given in Eq. (10) and (15) is given in Table 1.

4. Conclusion

To summarise, we have explored the consequences of applying the COE to random vector scattering matrices that incorporate the polarisation properties of light. When viewing the outgoing field in a single mode away from the backscattering direction, the polarisation state of the scattered field is uniformly distributed over the Poincaré sphere for different realisations of the scattering matrix. The average Mueller matrix is thus a pure depolariser. In the backscattering direction, the average Mueller matrix is only partially depolarising and the scattered fields are distributed non-uniformly on the Poincaré sphere, tending to focus around the incident polarisation state. The distributions for retardance and diattenuation associated with Jones matrices within \mathbf{S} are non-trivial. For a given instance of a scattering

Variable	α	Mean	Variance	Skewness	Kurtosis
D	1	$\frac{2}{3}$	$\frac{1}{18}$	$-\frac{2}{5}\sqrt{2}$	$\frac{12}{5}$
	2	$\frac{3}{4}$	$\frac{3}{80}$	$-\frac{2}{3}\sqrt{\frac{5}{3}}$	$\frac{65}{21}$
R	1	2	$4(\pi - 3)$	$\frac{3\pi^2 - 12\pi + 8}{4(\pi - 3)^{\frac{3}{2}}}$	$\frac{\pi^3 - 6\pi^2 - 12\pi + 66}{2(\pi - 3)^2}$
	2	$\frac{\pi^2 + 4}{2\pi}$	$\frac{\pi^4 - 48}{12\pi^2}$	$\frac{24\sqrt{3}(\pi^4 - 12\pi^2 + 16)}{(\pi^4 - 48)^{\frac{3}{2}}}$	$\frac{9(\pi^8 - 800\pi^4 + 7680\pi^2 - 3840)}{5(\pi^4 - 48)^2}$

Table 1: Statistics of diattenuation and retardance distributions. Retardance statistics were calculated using Eq. (10) and diattenuation statistics using Eq. (15).

matrix, it is most probable that a random scattering medium acts as a serial combination of a polarising filter followed by a half-wave plate with diattenuation and retardance vectors uniformly distributed on the Poincaré sphere.

220 As a model for random scattering matrices, the COE is clearly limited and is unable to describe anisotropic scattering. Nevertheless, compared to more sophisticated random matrix models, the COE is mathematically simple and may serve as a reference model for fully depolarising media. The task of exploring more general random matrix ensembles is left for future studies.

225 Appendix A. Alternate asymptotic derivation

In this section we outline an alternative derivation of Eq. (15). For large N , the elements of a matrix drawn from the COE can be treated as uncorrelated, zero-mean complex Gaussian random variables with variances given by [50]

$$\langle |S_{ij}|^2 \rangle \sim \frac{1 + \delta_{ij}}{N}. \quad (\text{A.1})$$

Let \mathbf{J} be a 2×2 sub-block of \mathbf{S} , and let $\mathbf{T} = \sqrt{N}\mathbf{J}$. Notably, \mathbf{T} has the same diattenuation as \mathbf{J} . By considering Eq. (A.1), it can be shown that \mathbf{T} has joint density given by

$$p(\mathbf{T}) \propto \exp\left(-\frac{1}{3-\alpha}\text{tr}(\mathbf{T}^\dagger\mathbf{T})\right). \quad (\text{A.2})$$

Taking a singular value decomposition of \mathbf{T} as in the main text and changing variables yields the density for the singular values of \mathbf{T} , s_1 and s_2 , which is given by

$$p(s_1, s_2) \propto s_1 s_2 |s_1^2 - s_2^2|^\alpha \exp\left(-\frac{1}{3-\alpha}(s_1^2 + s_2^2)\right). \quad (\text{A.3})$$

The probability density function for the diattenuation can therefore be calculated from the integral

$$p(D) \propto \int_0^\infty \int_0^\infty s_1 s_2 |s_1^2 - s_2^2|^\alpha \exp\left(-\frac{1}{3-\alpha}(s_1^2 + s_2^2)\right) \delta\left(D - \frac{|s_1^2 - s_2^2|}{s_1^2 + s_2^2}\right) ds_1 ds_2, \quad (\text{A.4})$$

which can be evaluated to yield the density given in Eq. (15).

Acknowledgements

This work was supported by the Royal Society (grant numbers RGF\R1\180052 and UF150335)

References

- [1] R. M. A. Azzam, R. Azzam, N. Bashara, *Ellipsometry and Polarized Light*, North-Holland, 1987.
URL <https://books.google.co.uk/books?id=db3vAAAAAAAJ>
- [2] A. Chrysostomou, P. W. Lucas, J. H. Hough, Circular polarimetry reveals helical magnetic fields in the young stellar object hh 135–136, *Nature* 450 (7166) (2007) 71–73. doi:10.1038/nature06220.
URL <https://doi.org/10.1038/nature06220>
- [3] M. R. Foreman, C. Macías Romero, P. Török, Determination of the three dimensional orientation of single molecules, *Optics Letters* 33 (2008) 1020–1022.
- [4] J. Chon, P. Zijlstra, M. Gu, Five-dimensional optical recording mediated by surface plasmons in gold nanorods, *Nature* 459 (2009) 410–413.
- [5] R. S. Gurjar, V. Backman, L. T. Perelman, I. Georgakoudi, K. Badizadegan, I. Itzkan, R. R. Dasari, M. S. Feld, Imaging human epithelial properties with polarized light-scattering spectroscopy, *Nature Medicine* 7 (11) (2001) 1245–1248. doi:10.1038/nm1101-1245.
URL <https://doi.org/10.1038/nm1101-1245>
- [6] J. Goodman, *Speckle Phenomena in Optics: Theory and Applications*, Roberts & Company, 2007.
URL <https://books.google.co.uk/books?id=TynXEcS0DncC>
- [7] A. Dogariu, R. Carminati, Electromagnetic field correlations in three-dimensional speckles, *Physics Reports* 559 (2015) 1–29. doi:<https://doi.org/10.1016/j.physrep.2014.11.003>.
URL <https://www.sciencedirect.com/science/article/pii/S0370157314004050>
- [8] M. Born, E. Wolf, *Principles of Optics: Electromagnetic Theory of Propagation, Interference and Diffraction of Light*, Elsevier Science, 2013.
URL <https://books.google.co.uk/books?id=HY-GDAAAQBAJ>

- [9] D. Eliyahu, Vector statistics of correlated Gaussian fields, *Physical Review E* 47 (1993) 2881–2892. doi:10.1103/PhysRevE.47.2881.
URL <https://link.aps.org/doi/10.1103/PhysRevE.47.2881>
- 260 [10] D. Eliyahu, Statistics of Stokes variables for correlated Gaussian fields, *Physical Review E* 50 (1994) 2381–2384. doi:10.1103/PhysRevE.50.2381.
URL <https://link.aps.org/doi/10.1103/PhysRevE.50.2381>
- [11] R. Barakat, Statistics of the Stokes parameters, *Journal of the Optical Society of America A* 4 (7) (1987) 1256–1263. doi:10.1364/JOSAA.4.001256.
265 URL <http://josaa.osa.org/abstract.cfm?URI=josaa-4-7-1256>
- [12] R. Barakat, The statistical properties of partially polarized light, *Optica Acta: International Journal of Optics* 32 (3) (1985) 295–312. arXiv:<https://doi.org/10.1080/713821736>, doi:10.1080/713821736.
URL <https://doi.org/10.1080/713821736>
- 270 [13] C. Brosseau, R. Barakat, E. Rockower, Statistics of the Stokes parameters for Gaussian distributed fields, *Optics Communications* 82 (3) (1991) 204–208. doi:[https://doi.org/10.1016/0030-4018\(91\)90445-J](https://doi.org/10.1016/0030-4018(91)90445-J).
URL <https://www.sciencedirect.com/science/article/pii/003040189190445J>
- [14] N. Hagen, Statistics of normalized Stokes polarization parameters, *Applied Optics* 57 (19) (2018) 5356–5363. doi:10.1364/AO.57.005356.
275 URL <http://ao.osa.org/abstract.cfm?URI=ao-57-19-5356>
- [15] P. F. Steeger, T. Asakura, K. Zocha, A. F. Fercher, Statistics of the Stokes parameters in speckle fields, *Journal of the Optical Society of America A* 1 (6) (1984) 677–682. doi:10.1364/JOSAA.1.000677.
280 URL <http://josaa.osa.org/abstract.cfm?URI=josaa-1-6-677>
- [16] L. Jin, M. Kasahara, B. Gelloz, K. Takizawa, Polarization properties of scattered light from macrorough surfaces, *Optics Letters* 35 (4) (2010) 595–597. doi:10.1364/OL.35.000595.
URL <http://ol.osa.org/abstract.cfm?URI=ol-35-4-595>
- 285 [17] A. Ghabbach, M. Zerrad, G. Soriano, S. Liukaityte, C. Amra, Depolarization and enpolarization DOP histograms measured for surface and bulk speckle patterns, *Optics Express* 22 (18) (2014) 21427–21440. doi:10.1364/OE.22.021427.
URL <http://www.opticsexpress.org/abstract.cfm?URI=oe-22-18-21427>
- [18] G. D. Lewis, D. L. Jordan, Remote sensing of polarimetric speckle, *Journal of Physics D: Applied Physics* 34 (9) (2001) 1399–1407. doi:10.1088/0022-3727/34/9/317.
290 URL <https://doi.org/10.1088/0022-3727/34/9/317>
- [19] F. Ulaby, K. Sarabandi, A. Nashashibi, Statistical properties off the Mueller matrix of distributed targets, *IEE Proceedings F Radar and Signal Processing* 139 (2) (1992) 136. doi:10.1049/ip-f-2.1992.0017.
295 URL <https://doi.org/10.1049/ip-f-2.1992.0017>

- [20] A. H. Hielscher, A. A. Eick, J. R. Mourant, D. Shen, J. P. Freyer, I. J. Bigio, Diffuse backscattering Mueller matrices of highly scattering media, *Optics Express* 1 (13) (1997) 441–453. doi:10.1364/OE.1.000441.
URL <http://www.opticsexpress.org/abstract.cfm?URI=oe-1-13-441>
- 300 [21] M. Sun, H. He, N. Zeng, E. Du, Y. Guo, S. Liu, J. Wu, Y. He, H. Ma, Characterizing the microstructures of biological tissues using Mueller matrix and transformed polarization parameters, *Biomedical Optics Express* 5 (12) (2014) 4223. doi:10.1364/boe.5.004223.
URL <https://doi.org/10.1364/boe.5.004223>
- 305 [22] S.-Y. Lu, R. A. Chipman, Interpretation of Mueller matrices based on polar decomposition, *Journal of the Optical Society of America A* 13 (5) (1996) 1106–1113. doi:10.1364/JOSAA.13.001106.
URL <http://josaa.osa.org/abstract.cfm?URI=josaa-13-5-1106>
- [23] J. Rehbinder, H. Haddad, S. Deby, B. Teig, A. Nazac, T. Novikova, A. Pierangelo, 310 F. Moreau, Ex vivo Mueller polarimetric imaging of the uterine cervix: a first statistical evaluation, *Journal of Biomedical Optics* 21 (7) (2016) 1 – 8. doi:10.1117/1.JBO.21.7.071113.
URL <https://doi.org/10.1117/1.JBO.21.7.071113>
- [24] M. Mozumder, J. Jagtap, P. Shukla, A. Pradhan, Images of depolarization power and retardance to study stages of dysplasia in human cervical tissues, in: A. P. Wax, V. Backman (Eds.), *Biomedical Applications of Light Scattering V*, Vol. 7907, International Society for Optics and Photonics, SPIE, 2011, pp. 186 – 196. doi:10.1117/12.875119.
URL <https://doi.org/10.1117/12.875119>
- 315 [25] Y. A. Ushenko, O. V. Dubolazov, A. O. Karachevtsev, Statistical structure of skin derma Mueller matrix images in the process of cancer changes, *Optical Memory and Neural Networks* 20 (2) (2011) 145–154. doi:10.3103/S1060992X1102010X.
URL <https://doi.org/10.3103/S1060992X1102010X>
- 320 [26] P. Yu, Q. Zhao, X. Hu, Y. Li, L. Gong, Tailoring arbitrary polarization states of light through scattering media, *Applied Physics Letters* 113 (12) (2018) 121102. arXiv: <https://doi.org/10.1063/1.5048493>, doi:10.1063/1.5048493.
325 URL <https://doi.org/10.1063/1.5048493>
- [27] Y.-Y. Xie, B.-Y. Wang, Z.-J. Cheng, Q.-Y. Yue, C.-S. Guo, Measurement of vector transmission matrix and control of beam focusing through a multiple-scattering medium based on a vector spatial light modulator and two-channel polarization holography, *Applied Physics Letters* 110 (22) (2017) 221105. arXiv:<https://doi.org/10.1063/1.4984209>, doi:10.1063/1.4984209.
330 URL <https://doi.org/10.1063/1.4984209>
- [28] S. Tripathi, R. Paxman, T. Bifano, K. C. Toussaint, Vector transmission matrix for the polarization behavior of light propagation in highly scattering media, *Optics Express*

- 335 20 (14) (2012) 16067–16076. doi:10.1364/OE.20.016067.
URL <http://www.opticsexpress.org/abstract.cfm?URI=oe-20-14-16067>
- [29] S. Rotter, S. Gigan, Light fields in complex media: Mesoscopic scattering meets wave control, *Reviews of Modern Physics* 89 (2017) 015005. doi:10.1103/RevModPhys.89.015005.
340 URL <https://link.aps.org/doi/10.1103/RevModPhys.89.015005>
- [30] Universality classes and fluctuations in disordered systems, *Proceedings of the Royal Society of London. Series A: Mathematical and Physical Sciences* 437 (1899) (1992) 67–83. doi:10.1098/rspa.1992.0047.
URL <https://doi.org/10.1098/rspa.1992.0047>
- 345 [31] C. W. J. Beenakker, Random-matrix theory of quantum transport, *Reviews of Modern Physics* 69 (1997) 731–808. doi:10.1103/RevModPhys.69.731.
URL <https://link.aps.org/doi/10.1103/RevModPhys.69.731>
- [32] S. Rothe, H. Radner, N. Koukourakis, J. W. Czarske, Transmission matrix measurement of multimode optical fibers by mode-selective excitation using one spatial light modulator, *Applied Sciences* 9 (1) (2019) 195. doi:10.3390/app9010195.
350 URL <https://doi.org/10.3390/app9010195>
- [33] S. F. Mingaleev, K. Busch, Scattering matrix approach to large-scale photonic crystal circuits, *Optics Letters* 28 (8) (2003) 619–621. doi:10.1364/OL.28.000619.
URL <http://ol.osa.org/abstract.cfm?URI=ol-28-8-619>
- 355 [34] N. Byrnes, M. R. Foreman, Symmetry constraints for vector scattering and transfer matrices containing evanescent components: Energy conservation, reciprocity, and time reversal, *Physical Review Research* 3 (2021) 013129. doi:10.1103/PhysRevResearch.3.013129.
URL <https://link.aps.org/doi/10.1103/PhysRevResearch.3.013129>
- 360 [35] M. Mishchenko, M. Mishchenko, L. Travis, A. Lacis, *Multiple Scattering of Light by Particles: Radiative Transfer and Coherent Backscattering*, Cambridge University Press, 2006.
URL <https://books.google.co.uk/books?id=ODfEI-2ykLsC>
- [36] P. Forrester, *Log-Gases and Random Matrices (LMS-34)*, London Mathematical Society Monographs, Princeton University Press, 2010.
365 URL <https://books.google.co.uk/books?id=C7z3Ng01b1gC>
- [37] G. Akemann, J. Baik, P. Di Francesco, *The Oxford Handbook of Random Matrix Theory*, Oxford University Press, 2018.
URL <https://books.google.co.uk/books?id=yq7YvQEACAAJ>
- 370 [38] S. Matsumoto, General moments of matrix elements from circular orthogonal ensembles, *Random Matrices: Theory and Applications* 01 (03) (2012) 1250005. doi:10.1142/s2010326312500050.
URL <https://doi.org/10.1142/s2010326312500050>

- [39] J. Perez, R. Ossikovski, Polarized Light and the Mueller Matrix Approach, Series in Optics and Optoelectronics, CRC Press, 2017.
375 URL <https://books.google.co.uk/books?id=yBVjDAAAQBAJ>
- [40] C. Brosseau, Fundamentals of Polarized Light: A Statistical Optics Approach, Wiley, 1998.
URL <https://books.google.co.uk/books?id=477vAAAAAAAJ>
- [41] S.-Y. Lu, R. A. Chipman, Homogeneous and inhomogeneous Jones matrices, Journal of the Optical Society of America A 11 (2) (1994) 766–773. doi:10.1364/JOSAA.11.000766.
380 URL <http://josaa.osa.org/abstract.cfm?URI=josaa-11-2-766>
- [42] W. A. Friedman, P. A. Mello, Marginal distribution of an arbitrary square submatrix of the S-matrix for Dyson’s measure, Journal of Physics A: Mathematical and General 18 (3) (1985) 425–436. doi:10.1088/0305-4470/18/3/018.
385 URL <https://doi.org/10.1088/0305-4470/18/3/018>
- [43] P. Pereyra, P. A. Mello, Marginal distribution of the S-matrix elements for Dyson’s measure and some applications, Journal of Physics A: Mathematical and General 16 (2) (1983) 237–254. doi:10.1088/0305-4470/16/2/007.
390 URL <https://doi.org/10.1088/0305-4470/16/2/007>
- [44] R. Horn, C. Johnson, Matrix Analysis, Cambridge University Press, 2012.
URL <https://books.google.co.uk/books?id=07sgAwAAQBAJ>
- [45] M. Mehta, Random Matrices, ISSN, Elsevier Science, 2004.
395 URL https://books.google.co.uk/books?id=Kp3Nx03_gMwC
- [46] A. Vannucci, A. Bononi, Statistical characterization of the Jones matrix of long fibers affected by polarization mode dispersion (pmd), Journal of Lightwave Technology 20 (5) (2002) 783.
URL <http://jlt.osa.org/abstract.cfm?URI=jlt-20-5-783>
- [47] D. Zwillinger, A. Jeffrey, Table of Integrals, Series, and Products, Elsevier Science, 2007.
400 URL <https://books.google.co.uk/books?id=aBgFYxKHUjsC>
- [48] A. P. Mosk, A. Lagendijk, G. Lerosey, M. Fink, Controlling waves in space and time for imaging and focusing in complex media, Nature Photonics 6 (5) (2012) 283–292. doi:10.1038/nphoton.2012.88.
405 URL <https://doi.org/10.1038/nphoton.2012.88>
- [49] M. Cvitkovi’c, A.-S. Smith, J. Pande, Asymptotic expansions of the hypergeometric function with two large parameters—application to the partition function of a lattice gas in a field of traps, Journal of Physics A: Mathematical and Theoretical 50 (26) (2017) 265206. doi:10.1088/1751-8121/aa7213.
410 URL <https://doi.org/10.1088/1751-8121/aa7213>

- [50] W. Friedman, P. Mello, Information theory and statistical nuclear reactions II. Many-channel case and Hauser-Feshbach formula, *Annals of Physics* 161 (2) (1985) 276–302.
doi:[https://doi.org/10.1016/0003-4916\(85\)90081-8](https://doi.org/10.1016/0003-4916(85)90081-8).
URL <https://www.sciencedirect.com/science/article/pii/0003491685900818>